

HANDLING OF LARGE BLOCK OF HIGH RESOLUTION SPACE IMAGES

Ricardo M. Passini (*), Allan Blades (*), Karsten Jacobsen (**)
(*) BAE SYSTEMS, rpassini@adrinc.com; ablades@adrinc.com
(**) University of Hannover, jacobsen@ipi.uni-hannover.de

Keywords: QuickBird, IKONOS, Scene Orientation, Block Adjustment

ABSTRACT:

A large block of QuickBird Basic Imagery has been analyzed for optimal control distribution and scene ties. This has been done by three dimensional adjustment a block of Basic Imagery using satellite ephemerides and attitude (quaternion) data along with ground control points (GCPs). Different GCPs configuration and check points were used to assess the achieved accuracy. Alternative a transformation to a plane with constant height followed by a two dimensional block adjustment was used for a small block of IKONOS images. Only the horizontal coordinates of the ground control points and check points have been available, so the SRTM – height model was used for the third dimension.

1. INTRODUCTION

Digital Orthophotos is the most commonly and widely used mapping product in these days. The processes involved for its generation have been conveniently automated to a large degree what makes it to a very economical attractive alternative to the traditional line mapping. It has nearly the metric characteristics of maps plus the unreduced pictorial information contents. The time consuming interpretation of vector mapping is not required. In other words, the cartographic symbols are replaced by the image of the same features without any generalization.

Modern high resolution satellite images (i.e., IKONOS, QuickBird, OrbView-3) provides simultaneous panchromatic and multispectral image acquisition and almost progressive continuous orbit coverage, allowing a large area coverage in minimum time. A permanent platform rotation allows the line exposures to be made parallel with the x-axis of cartographic systems simplifying the automation on the production of the orthomosaics.

The achieved accuracy in an orthophoto depends mainly on the accuracy of the orientation parameters of the used imagery and on the accuracy of the digital elevation model (DEM). On the other hand the accuracy of the orientation depends on the used mathematical model, the accuracy, number and distribution of GCPs. The number and required distribution of GCPs is determined by the used mathematical model and the sensor. The present investigation concentrates on the study of the orientation accuracy using mainly two orientation methods and different number and distribution of GCPs. For that purpose a blocks of high resolution panchromatic QuickBird images was used. It is composed of 40 images from 6 contiguous orbits. GCPs were manually transferred from higher resolution, accurate stereoscopic oriented panchromatic aerial photos. The orientation accuracy of the aerial photos relative to check points shall be in

the range of 1.0 m. Figure 2 shows the block along with the GCPs distribution

In relation to the used orientation models, two were employed, namely the space resection based on the satellite ephemerides and the attitude quaternions, and a second method that transforms the images to a plane with constant height followed by a two dimensional block adjustment based on combined shift or up to 6 affine parameters. The first method is implemented in BAE SYSTEMS Socet Set (MST) and the second was derived at the University of Hannover. The first part of observations were made using the Socet Set Systems through its module multisensor triangulation (MST), almost progressive continuous orbit coverage, allowing in such way large area coverage in minimum time while for the second part the Hannover program DPLX was used.

2. ORIENTATION MODELS

The bundle model is based on the widely known collinearity condition equation of CCD-lines. The exterior orientation parameters of each CCD-line are different, but the relation of the exterior orientation to the satellite orbit is only changing slightly. Hence for the classical CCD-line cameras, the attitudes are not changing in relation to the satellite orbit. So for an image it is possible to consider time (space) dependent attitude parameters. Taking into consideration the general information about the view direction of the satellite, the “in track and across track view angles” (included within the QuickBird *.imd-file) and knowing that in a basic imagery the effects of the high frequency movements have been eliminated, then the effects of the low frequency motions of the platform can be modeled by self calibration via additional parameters.

The additional parameters been used by the Hannover orientation program BLASPO are checked for numerical stability, statistical significance and

reliability in order to justify their presence and to avoid over-parameterization. The program automatically reduces the parameters specified by dialogue to the required group by a statistical analysis based on a combination of Student-test, the correlation and total correlation. This guarantees that not over-parameterization occurs. In that case an extrapolation outside the area covered by control points does not become dangerous.

2.1 Bundle Orientation using ephemeris and Attitude Quaternion

The camera sensor model distributed by DigitalGlobe contains five coordinates systems, namely:

earth coordinates (EC), spacecraft coordinates (SC), camera coordinates (CC), detector coordinates (DC) and image coordinates (IC). Definitions and details regarding these systems can be found in DigitalGlobe QuickBird Imagery Product Guide.

The data contained in the ephemeris file are sample mean and covariance estimates of the position of the spacecraft system relative to the earth centered fixed (ECF) system. These files are produced for a continuous image period, e.g., an image or strip. The attitude file contains sample mean and covariance estimates of the attitude space craft system relative to the ECF system. These files are produced for a continuous imaging period, e.g., a snap or strip, and span the period for at least four seconds before the start of imaging and after the end of imaging. The instantaneous spacecraft attitude is represented by four-element quaternion. It describes a hypothetical 3D rotation of the spacecraft frame with respect to the ECF frame. Any such a 3D rotation can be expressed by a rotation angle, θ and an axis of rotation given by unit vector components (ξ_x, ξ_y, ξ_z) in the ECF frame. The sign and rotation angle follows the right-hand rule. Finally the quaternion $(q1, q2, q3, q4)$ is related to θ and (ξ_x, ξ_y, ξ_z) by:

$$\begin{aligned} \mathbf{q1} &= \xi_x \sin(\theta/2) \\ \mathbf{q2} &= \xi_y \sin(\theta/2) \\ \mathbf{q3} &= \xi_z \sin(\theta/2) \dots (1) \\ \mathbf{q4} &= \cos(\theta/2) \end{aligned}$$

The image lines in the Basic Imagery product are sampled at a constant rate. This means that the imaging time can be computed directly from the given data avgLineRate (Average Line Rate) and firstLineTime (First Line Time) with no approximations:

$$t = \tau / \text{avgLineRate} + \text{firstLineTime} \quad (2)$$

One point on the imaging ray is the perspective center of the virtual camera at time t. The coordinates of the perspective center in the spacecraft coordinate system are constant and given data. In matrix notation:

$$\mathbf{C}_S = (C_X, C_Y, C_Z)^T \dots (3)$$

where C_X, C_Y and C_Z are values of the camera calibration file (*.geo File). It is possible to locate the origin of the spacecraft coordinate system in the ECF system at a time t by interpolating the position time series in the ephemeris file. Let us call this position $S_E(t)$. Likewise, we can find the attitude of the spacecraft coordinate system at a time (t) in the ECF system by interpolating the quaternion time series in the attitude file. This quaternion, $\mathbf{q}_E^S(t)$, represents the rotation from the ECF system to the spacecraft body system at time t. Then using quaternion algebra, the position of the perspective center at time t in the ECF coordinate system is:

$$\mathbf{C}_E(t) = (\mathbf{q}_E^S(t))^{-1} \mathbf{C}_S \mathbf{q}_E^S(t) + S_E(t), \quad \text{or}$$

$$\mathbf{C}_E(t) = \mathbf{q}_E^S(t) \mathbf{C}_S (\mathbf{q}_E^S(t))^{-1} + S_E(t) \dots (4)$$

Alternatively, computing $\mathbf{R}_S^E(t)$, the rotation matrix from the given quaternions $\mathbf{q}_E^S(t)$ for time (t) as a rotation from the spacecraft body to the ECF, then (4) above can be expressed by:

$$\mathbf{C}_E(t) = \mathbf{R}_S^E(t) \mathbf{C}_S + S_E(t) \dots (5)$$

Expressions (4) and (5) are the position of the projection center at the instant (t) expressed in the ECF coordinate system that may corresponds to a position of a GCP in the image. In this way it can be replaced in the colinearity equation above for the position (line j) that corresponds to a time (t).

For any column and row measurement (c, r) of a pixel in the image, the corresponding position of the image point in the detector coordinate system (relative to the center of the lowest numbered pixel in the detector) is:

$$X_D = 0$$

$$Y_D = -c * \text{detPitch},$$

with detPitch being the distance (in mm) between centers of adjacent pixels in the array

To convert these detector coordinates to camera coordinates, it is necessary to apply the rotation and translation given by the following equations:

$$X_C = \cos(\text{detRotAngle}) * X_D - \sin(\text{detRotAngle}) * Y_D + \text{detOriginX}$$

$$X_C = \sin(\text{detRotAngle}) * X_D + \cos(\text{detRotAngle}) * Y_D + \text{detOriginY} \dots (7)$$

$$Z_D = C \text{ (Virtual Principal Distance)}$$

rotation from the spacecraft body to the ECF, then (5) above can be expressed by:

$$\mathbf{C}_E(t) = \mathbf{R}_S^E(t) \mathbf{C}_S + S_E(t) \dots (6)$$

Expressions (5) and (6) are the position of the projection center at the instant (t) expressed in the ECF coordinate system that may corresponds to a position of a GCP in the image. In this way it can be replaced in expressions (1) above for the position (line j) that corresponds to a time (t).

For any column and row measurement (c, r) of a pixel in the image, the corresponding position of the image point in the detector coordinate system (relative to the center of the lowest numbered pixel in the detector) is:

$$X_D = 0$$

$$Y_D = -c \cdot \text{detPitch},$$

with detPitch being the distance (in mm) between centers of adjacent pixels in the array

To convert these detector coordinates to camera coordinates, it is necessary to apply the rotation and translation given by the following equations:

$$X_C = \cos(\text{detRotAngle}) \cdot X_D - \sin(\text{detRotAngle}) \cdot Y_D + \text{detOriginX}$$

$$Y_C = \sin(\text{detRotAngle}) \cdot X_D + \cos(\text{detRotAngle}) \cdot Y_D + \text{detOriginY} \dots \dots \dots (6)$$

$$Z_D = C \text{ (Virtual Principal Distance)}$$

in the linear detector array, in the camera coordinates system, in mm. detRotAngle, detOriginX and detOriginY are included in the calibration data file (*.geo).

As Basic Imagery do not have lens distortion, the corrected image point is identical to the measured image point, hence:

$$\begin{aligned} X_C' &= X_C \\ Y_C' &= Y_C \\ Z_C' &= Z_C \end{aligned} \quad (7)$$

The unit vector w_C that is parallel to the external ray in the camera coordinate system is just the position of (X_C', Y_C', Z_C') relative to the perspective center at $(0, 0, 0)$, normalized by its length. In matrix notation, this vector is:

$$W_C = (X_C', Y_C', Z_C')^T \text{ and } w_C = W_C / \| W_C \| \quad (8)$$

It is possible to convert this vector at first to the spacecraft coordinate system and then to the ECF system. The unit quaternion for the attitude of the camera coordinate system, i.e., the quaternion for the rotation of spacecraft frame into the camera frame $q_{S_C}^C$, is in the geometric calibration file (*.geo). Then, using quaternion algebra

$$w_E = q_{S_C}^E(t)^{-1} q_{S_C}^S^{-1} w_C q_{S_C}^S q_{S_C}^E(t) \quad \text{or}$$

$$w_E = q_{S_C}^E(t) q_{S_C}^S w_C (q_{S_C}^S(t) q_{S_C}^E)^{-1}$$

or using matrix algebra,

$$w_E = R_{S_C}^E(t) R_{S_C}^S w_C \dots \dots \dots (9)$$

The resulting multiplication matrix $R_{S_C}^E(t)$ has form (10) with:

$$[R_{S_C}^E(t)]^T = (R_{S_C}^S(t) R_{S_C}^S)^T =$$

$$\frac{1}{\omega^2 + a(t)^2 + b(t)^2 + c(t)^2} \begin{bmatrix} \omega^2 + a(t)^2 - b(t)^2 - c(t)^2 & 2a(t)b(t) + 2\omega c(t) & 2a(t)c(t) - 2\omega b(t) \\ 2a(t)b(t) - 2\omega c(t) & \omega^2 - a(t)^2 + b(t)^2 - c(t)^2 & 2b(t)c(t) + 2\omega a(t) \\ 2b(t)c(t) + 2\omega b(t) & 2b(t)c(t) - 2\omega a(t) & \omega^2 - a(t)^2 - b(t)^2 + c(t)^2 \end{bmatrix} \dots \dots \dots (10)$$

ω : constant term, being a function of both scalars $q_{S_C}^E$ (4) and $q_{S_C}^S$ (4)

$a(t); b(t); c(t)$: Are elements of the instantaneous rotation matrix $[R_{S_C}^E(t)]^T$ also function of the quaternions $q_{S_C}^E(t)$ for the instant (t) and $q_{S_C}^S$. equation (10) can in this way be used in the bundle orientation.

The program system Multi Sensor Triangulation (MST) of BAE SYSTEMS's SOCET SET uses this approach for QuickBird Imagery.

2.2. Transformation to a Plane with Constant Height followed by a two Dimensional Block Adjustment

The three-dimensional adjustment requires a sufficient number of control points, leading to a combined resection or a sufficient image overlap enabling the spatial connection like in the case of a standard aerial triangulation. This overlap usually not exists, requiring a reduction of the three-dimensional case to a two-dimensional solution, corresponding to the classical Anblock triangulation. If no images transformed to a plane with constant height (like QuickBird OR-Standard or IKONOS Geo) are given, such a product should be generated based on the existing sensor orientation. It can be made with rational polynomial coefficients (RPCs) (Grodecki 2001) or using the image geometry described before. A simple transformation to a plane with constant height is leading to errors in the horizontal location caused by the height difference of the actual point against the average height.

$$DL = \Delta h \cdot \tan v \quad (11)$$

error in location caused by Δh and incidence angle v

It requires the "terrain relief correction". If no height of the required tie and control point is given, this has to be interpolated from a DEM. With nearly global coverage the SRTM C-band DEM can be used for images with limited incidence angle. Its standard deviation for the height in open and flat areas of approximately 4m (Jacobsen 2005) is causing in the average discrepancies below 1m if the incidence angle is not exceeding 14°. The interpolation within the

DEM requires the correct location which is not given in advance, so an iteration is required (approximate location \rightarrow approximate height \rightarrow better location \rightarrow better height \rightarrow . . .). If the tie and control points are not located in a position with remarkable terrain inclination, the iterative height interpolation can be based on the direct sensor orientation of the satellite. Only if such locations cannot be avoided, the iteration has to include also the position improvement by combined transformation to the control points. The iterative terrain relief correction can be based on a geometric reconstruction or RPCs (Büyüksalih, Jacobsen 2005).

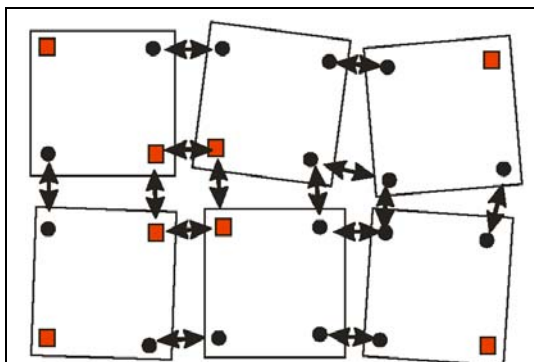


Fig. 1: basic principle of Anblock adjustment
 small square = control point
 circle = tie point

Figure 1 shows the basic principle of an Anblock adjustment – the two-dimensional images are connected by tie points and together they are related to some control points. The classical Anblock adjustment is based on a combined affine transformation, for each photo the 6 affine parameters have to be adjusted. 6 unknowns for each photo require a sufficient control point distribution. So it leads to numerical problems if the control point shown in the center of figure 1 is not available. On the other hand it has to be analyzed if really 6 unknowns are necessary for the matching of projected space images. In Büyüksalih, Jacobsen 2005 it has been shown, 6 parameters are required for a sub-pixel accuracy of QuickBird images while IKONOS images could be oriented with just shift parameters. By this reason such a combined orientation of a block of space photos has to be flexible with the number of used unknowns and like usually required, the significance and correlation of unknowns has to be checked.

3. Experimental Test

3.1. Block Adjustment using Ephemerides and Attitude Quaternion

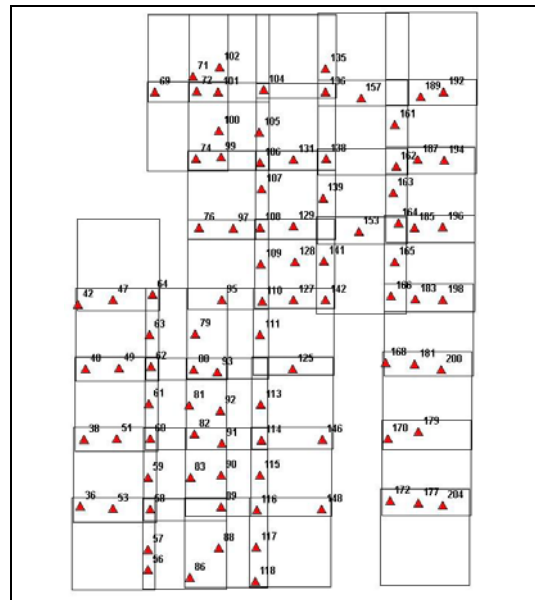


Fig. 2a :Full control distribution

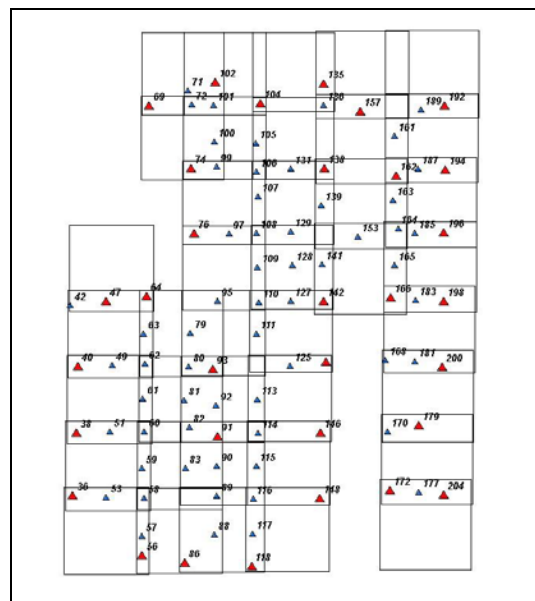


Fig. 2b: Perimeter control and randomly distributed GCPs in the center of the block

Figure 2 shows the foot print of the block of QuickBird images along with the location and distribution of the GCPs. The maximum number (case A) of used GCPs (89) in the experiments is shown in Figure 2a. Also adjustments with reduced numbers of GCPs were tested. For the study, this correspond to the

case B (perimeter control and randomly distributed GCPs in the center of the Block, Fig 2b), case C (perimeter control only), case D (relaxed perimeter control) and case E (GCPs only in the block corners). On each case (other than in case A), the remaining GCPs were used as a check points. The mayor inconveniences for the realization of the project represented the identification and transferring of the GCPs and check points. First of all the area of interest is mountainous and jungle with a huge and dense canopy typical of an equatorial area. Considerably time difference (3 years) between the reference aerial images and the recently acquired QuickBird scenes made it difficult to extract corresponding details. Illumination, seasonal differences, and image inclination imposed worse challenges to the operation.

Case	GCP	SX	SY	check points	RMSE _x	RMSE _y
A	89	0.52	0.53	-	-	-
B	33	0.45	0.44	56	1.77	2.59
C	25	0.35	0.35	64	1.94	2.72
D	9	0.33	0.34	80	3.42	4.21
E	5	0.24	0.26	84	5.27	6.93

Table 1: achieved results - use of different numbers of control points

SX,SY = MSE discrepancies at control points
 RMSE_x, y = discrepancies at check points

From Table 1 and 2 one clearly notice that with a reduced number of control points there is a better fitting of the block to the control but the absolute accuracy of the block identified at independent check points deteriorates very quickly reaching non tolerable values for control only in the block corners (Case E).

Case	GCP	DX max	DY max	check points	DX max	DY max
A	89	2.51	-2.1	-	-	-
B	33	1.22	-1.42	56	-4.7	7.2
C	25	1.12	1.12	64	5.6	8.3
D	9	1.12	0.92	80	8.8	-16.8
E	5	0.53	0.59	84	16.9	-20.4

Table 2: maximal discrepancies at control (left) and check points (right) based on different numbers of control points

Case	GCP	SX	SY	ΔX_{max}	ΔY_{max}
A	89	0.21	0.25	-2.53	-4.93
B	33	0.19	0.23	2.51	-4.56
C	25	0.16	0.22	2.48	-1.50
D	9	0.16	0.21	2.45	-1.48
E	5	0.15	0.20	2.06	-1.35

Table 3: internal accuracy at tie points

Table 3 shows the behavior of the block in terms of achieved internal accuracy based on statistics on its tie points. It shows a better internal relative fitting between contiguous images for more relaxed control. This is shown in the SX and SY and on the maximal residuals. Nevertheless, the reached maximal errors,

especially for the full controlled block suggest the presence of not yet detected gross errors among the image observations (i.e., in tie and/or transferred GCPs).

3.2. Two Dimensional Block Adjustment

The two-dimensional block adjustment could not be finished up to the dead line, but a smaller block of 4 IKONOS images has been handled. For the tie points, height values are required for a two-dimensional block adjustment. Only the SRTM C-band DEM has been available, having an accuracy in the range of 4m for flat and open terrain (Jacobsen 2005), but the area is mountainous and mainly covered by forest. So for tie points located in small clear cuts, the height value of the top of the trees has been interpolated and larger vertical discrepancies can be expected. The used IKONOS scenes do have incidence angles up to 26°. The tangent of the incidence multiplied with the 4m accuracy leads to 1.6m, which has to be doubled because of opposite view directions of overlapping scenes. Enough control points have been available for the orientation of the individual scenes based on rational polynomial coefficients and only a shift in X and Y for the bias correction. This resulted in the average in root mean square discrepancies at the control points (6 points in the average) of +/-1.21m for X and +/-2.79m for Y. The quite higher discrepancies in the Y-direction can be explained by the influence of the point heights. The point identification has an accuracy of 0.5 pixels = 0.5 m.

The determination of the tie point height requires an iteration. At first a simple affinity transformation of the pixel coordinates to control points was leading to rough ground coordinates – used for the interpolation of the height values. With these height values improved ground coordinates have been computed by rational polynomial coefficients – used again for the interpolation. For a nadir angle of 26° 4 to 5 iterations are required. The resulting ground coordinates of the tie points have been used for a block adjustment. The good internal accuracy of IKONOS-images required only a shift of the scenes in X and Y, a higher number of unknowns did not lead to improved results.

The internal accuracy of the block computation can be checked by the comparison of overlapping scenes, the results can be seen in figure 3a up to 3d and in table 4.

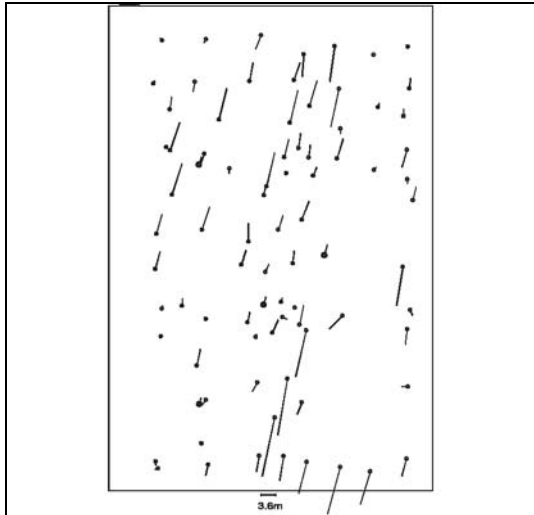


Fig. 3a discrepancies at tie points of 2 overlapping terrain relief corrected IKONOS-scenes

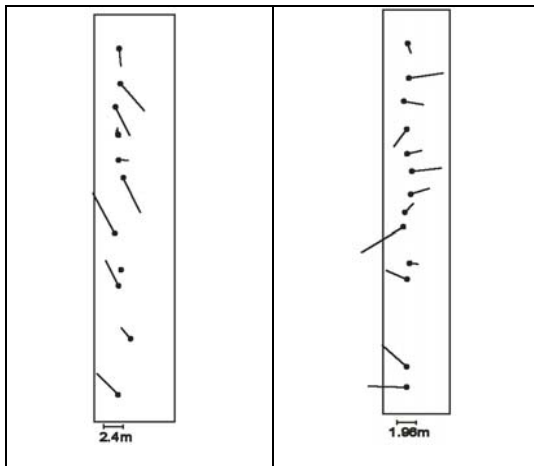


Fig. 3b and 3c discrepancies at tie points of 2 overlapping terrain relief corrected IKONOS-scenes

The transformation of overlapping scenes to each other shows larger discrepancies than the block adjustment itself, caused by the view from opposite direction enlarging the influence of the limited height accuracy of the used DEM. The coordinate component across the base direction (y-parallax) is independent upon the point height and this is limited in the root mean square average to 0.89m; that means to sub-pixel accuracy. Reverse this can be used for the estimation of the vertical accuracy respecting the individual height to base relation of the scene combinations – leading to a root mean square vertical accuracy of 6.2m. Under the condition of a mountainous terrain and the influence of neighbored forest this is a satisfying result for the SRTM C-band DEM, but it is not sufficient for the accuracy potential of the very high resolution space images. Under given condition,

the nadir angle should not exceed 10° to limit the influence of the used DEM to 1m or 1 pixel.

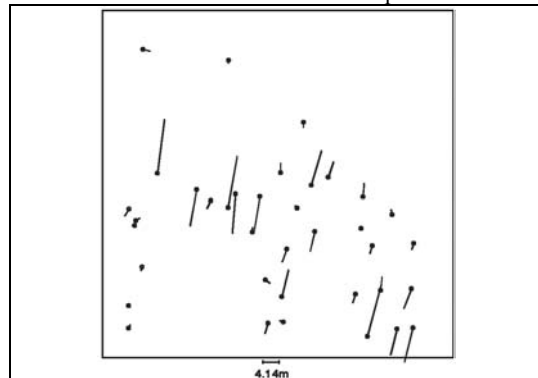


Fig. 3d discrepancies at tie points of 2 overlapping terrain relief corrected IKONOS-scenes

RMSX	RMSY	RMSbase	RMSacross
1.28m	4.95m	5.05m	0.95m
1.82m	2.95m	3.40m	0.65m
2.48m	1.23m	2.50m	1.18m
1.32m	5.70m	5.82m	0.67m

Table 4: internal accuracy of IKONOS block – comparison of overlapping scenes

CONCLUSION

A three-dimensional adjustment of a block of space images having only limited overlap is not leading to a real reduction of the number of required control points like shown with the problems of the reduced number of control points. The block adjustment should be done only in the X- and Y-plane after terrain relief correction. For the terrain relief correction a sufficient DEM is required. At the small block of IKONOS-scenes the influence of the limited vertical accuracy became obvious especially because of the larger nadir angles. If the nadir angles do not exceed 10° , the SRTM C-band DEM can be used for reaching satisfying results.

REFERENCES

- Büyüksalih, G., Jacobsen, K., 2005: Optimized Geometric Handling of High Resolution Space Images, ASPRS annual convention Baltimore, 2005, on CD
- Grodecki, J. (2001): IKONOS Stereo Feature Extraction – RPC Approach, ASPRS annual conference St. Louis, 2005, on CD
- Jacobsen, K. 2005: DEMs based on space images versus SRTM height models, ASPRS annual convention Baltimore, 2005, on CD
- Toutin, T., 2003: Block Adjustment of Landsat 7 ETM+ Images of Mountainous Areas, PERS 2003, pp1341 - 1349